

## **Effect of K<sub>2</sub>O/SiO<sub>2</sub> Ratio on the Crystallization of Leucite in Silicate-Based Glasses**

**Pat SOOKSAEN<sup>1,2\*</sup>, Janjira BOONMEE<sup>1</sup>, Chaiyaporn WITPATHOMWONG<sup>1</sup>  
and Somthida LIKHITLERT<sup>1</sup>**

<sup>1</sup>*Department of Materials Science and Engineering, Faculty of Engineering and Industrial Technology, Silpakorn University, Nakhon Pathom, 73000, Thailand*

<sup>2</sup>*Center of Excellence for Petroleum, Petrochemicals and Advanced Materials, Chulalongkorn University, Bangkok, 10330, Thailand*

### **Abstract**

Leucite-based glass-ceramics were prepared by controlled crystallization of suitable glass compositions to give required crystalline phase/s. Three glass batches in the system SiO<sub>2</sub> - K<sub>2</sub>O - NaO<sub>2</sub> - Al<sub>2</sub>O<sub>3</sub> - TiO<sub>2</sub> - CaO were prepared by varying K<sub>2</sub>O/SiO<sub>2</sub> ratio, then melted and quenched. Glasses were characterized for onset of crystallization temperatures by differential thermal analysis (DTA), and heat treatments were carried out from 850 – 1000°C for 4 hours for controlled crystallization of leucite phase. Physical, chemical and crystal structure characterizations were carried out using X-ray diffraction (XRD), Fourier transform infrared spectroscopy (FT-IR) and scanning electron microscopy (SEM). XRD found leucite as a major phase in all heat treatment temperatures. Increasing the heat treatment temperature as well as increasing the amount of K<sub>2</sub>O/SiO<sub>2</sub> ratio caused the amount of leucite phase to increase also. The silicate chain structure was found from FT-IR analysis, which confirmed the appearance of leucite phase. SEM indicated that increasing K<sub>2</sub>O/SiO<sub>2</sub> ratio in the glass batch led to a slight increase in the crystal size, and also a slight change in the morphology of the leucite phase. Glass with the highest K<sub>2</sub>O/SiO<sub>2</sub> ratio in this study, when heat-treated at 1000°C, showed an increased amount of secondary phase/s as opposed to the main leucite phase according to XRD data.

**Key words:** Leucite, Quenching, Heat treatment, Glass-ceramics, X-ray diffraction

### **Introduction**

Dental porcelain is a ceramic material which is currently used in dentistry, especially where aesthetics is needed. It has traditionally been made use of in the construction of artificial teeth for dentures, crowns and bridges.<sup>(1-3)</sup> From the 1980s onward, the use of ceramics has been extended to include veneers, inlays/onlays, crowns and bridges.<sup>(2)</sup> As people retain their teeth for much longer than in the past, the need for aesthetically acceptable restorations is continuing to increase. Dental porcelain is chemically very stable, and provides excellent aesthetics that do not deteriorate with time. The thermal properties are similar to those of enamel and dentine.<sup>(1-4)</sup> Although the compressive strength of dental porcelain is high (350 – 550 MPa), its tensile strength is very low (20 – 60 MPa), which is typical of a brittle solid. The material, being primarily a glass, lacks any fracture toughness.<sup>(3,5)</sup> Glasses are extremely sensitive to the presence of surface microcracks, and this represents one of the major drawbacks in the use of dental porcelain.<sup>(1,3,6)</sup>

Leucite (KAlSi<sub>2</sub>O<sub>6</sub>) is used as a major crystalline phase in a new generation of dental porcelains for all-ceramics restorations.<sup>(1)</sup> Leucite was initially introduced into dental porcelains to raise the composite coefficient of thermal expansion. In the last few years, it was found that the presence of leucite with suitable size range also improves fracture toughness. A reversible temperature dependent cubic to tetragonal leucite phase transformation occurs around 620–625°C.<sup>(7, 8)</sup> For dental porcelains this transformation occurs in the range of 400–600°C. Leucite transformation leads to a reversible volume change, from low temperature tetragonal to the high temperature cubic leucite. Typical leucite volume fractions for leucite containing dental porcelains vary between 17 and 45% of tetragonal leucite in a glassy matrix.<sup>(6, 7)</sup> Multiple firings, isothermal heat treatments and cooling can modify this content.<sup>(6, 7, 9)</sup> Many of the current commercial dental porcelains are produced with larger leucite crystal sizes (~5-10 μm). The thermal expansion mismatch between the leucite crystals and the glass matrix developed during leucite transformation often causes microcracking

---

\* Corresponding author E-mail: pat@su.ac.th

around larger, non-uniform leucite crystals and clusters.<sup>(6, 7, 10, 11)</sup> This would lead to a decrease of fracture toughness.

Leucite crystals can be prepared via glass-ceramic route employing a conventional glass forming methods. Glass ceramic is a polycrystalline solid prepared by the controlled crystallization of a glass.<sup>(4, 9, 11, 12)</sup> It is a multiphase solid containing a residual glass phase with a finely dispersed crystalline phase or phases. It usually gives complex, large, fine-grained microstructure and pore-free body.<sup>(4, 9, 13)</sup> The number of crystals, the growth rate as well as the size and morphology and the distribution are carefully controlled by the heat treatment process. Two important processes in the crystallization involve crystal nucleation and crystal growth and, generally, a fine grained microstructure is desirable for improved mechanical strength and wear.<sup>(9, 14-16)</sup> of glass-ceramics. To ensure a high strength for the glass ceramic it is also important that the crystals are numerous and are uniformly distributed throughout the glassy phase.

The first glass ceramic employed in dentistry was introduced by MacCulloch in 1968 for the construction of denture teeth, and was based on the  $\text{Li}_2\text{O}.\text{ZnO}.\text{SiO}_2$  system. Later, commercial glass-ceramic material called Dicor was used for fixed prostheses and contained filler particles of a type of crystalline mica (at 55 vol%).<sup>(9)</sup> More recently, glass ceramic containing 70 vol% crystalline lithium disilicate filler has been commercialized for dental use (Empress 2).<sup>(17)</sup> The leucite-containing ceramics used in restorations have a flexural strength of the order of 30 – 40 MPa. The leucite-containing glass-ceramics, however, have flexural strengths of up to 120 MPa. They can be manufactured for dental applications by controlled crystallization of glasses, which generally involves the melting, forming and cooling of glasses to form appropriate shapes or powders that are subsequently reheated to promote crystallization via a nucleation and growth process.

This article investigated three glass compositions based on a similar composition studied by Cattell, *et al.*<sup>(10)</sup> Different weight ratios of  $\text{K}_2\text{O}$  to  $\text{SiO}_2$  were chosen to study for their phase evolution and the related microstructures under different heat treatment temperatures. It was initially expected that the glass batches proposed in this study would result in the crystallization of more leucite phase with increasing  $\text{K}_2\text{O}/\text{SiO}_2$  ratio. To date, the effect of  $\text{K}_2\text{O}/\text{SiO}_2$  ratio on the phase evolution in glass-

ceramics has not been investigated in any other scientific article and the results found in this work could lead to creating glass-ceramics with better properties for potential dental applications.

## Materials and Experimental Procedures

### Glass Preparation

The compositions selected for the study were based on a similar composition proposed by Cattell, *et al.*<sup>(10)</sup> For each glass composition (Table 1), the batch was prepared according to the calculation to give approximately 150 g total weight. The appropriate ratios of raw materials;  $\text{SiO}_2$ ,  $\text{K}_2\text{CO}_3$ ,  $\text{Na}_2\text{CO}_3$ ,  $\text{Al}_2\text{O}_3$ ,  $\text{CaCO}_3$  and  $\text{TiO}_2$ , all with purity  $\geq 99\%$ , were weighed out to a precise balance and mixed via ball milling in HDPE bottle for 2 hours the batch was then transferred to an alumina crucible for melting. The glass batch was held at  $950^\circ\text{C}$  for 1 hour to decompose carbonates; subsequently, melting was carried out in an electric furnace for 4 hours at  $1300^\circ\text{C}$ . After melting, the glass melt was taken out directly from the furnace and was quenched rapidly into water bath to prevent devitrification (i.e. uncontrolled crystallization). Glass frit was crushed and ground to give fine glass powders and sieved through  $106\ \mu\text{m}$  for further processing.

**Table 1.** Glass batches melted in weight% oxides

Glass	Oxide (weight %)					
	$\text{SiO}_2$	$\text{K}_2\text{O}$	$\text{Na}_2\text{O}$	$\text{Al}_2\text{O}_3$	$\text{CaO}$	$\text{TiO}_2$
Glass A	65	10	5	15	3	2
Glass B	63	12	5	15	3	2
Glass C	61	14	5	15	3	2

### Differential Thermal Analysis

Differential Thermal Analysis (DTA) was used to establish chemical and physical transformation temperatures such as the glass transition temperature ( $T_g$ ), onset of various crystallization temperatures and melting temperature. In this study, DTA of as-quenched glasses A, B and C was performed on a NETZSCH STA 449C (TGA-DTA). For each DTA run, approximately 45 mg of a fine glass powder was filled into a small alumina crucible and heated in air from room temperature to  $1200^\circ\text{C}$  with a heating rate of  $15^\circ\text{C}/\text{minute}$  against an  $\text{Al}_2\text{O}_3$  control powder.

## *Effect of K<sub>2</sub>O/SiO<sub>2</sub> Ratio on the Crystallization of Leucite in Silicate-Based Glasses*

### **Crystallization of Glasses**

Samples were prepared by uniaxial pressing of fine glass powders to form pellets of 10 mm diameter and 3 mm thickness using a pressure of 150 MPa and 30 seconds holding time. Crystallization temperatures were established from the DSC data. Single-step heat treatments to crystallize these glasses were carried out at 850, 900, 950 and 1000°C for 4 hours using a heating/cooling rate of 5°C/minute.

### **X-ray Diffraction**

X-ray Diffraction (XRD) was used to identify phases present in the crystallized glass samples and also to study the crystal structure of the leucite (KAlSi<sub>2</sub>O<sub>6</sub>) phase. Samples were analyzed as bulk on a smooth surface. The analyses were performed at room temperature on a Bruker AXS D8 Discover from 10° to 70° 2θ with a scan speed of 2°/minute and step size 0.02° using Cu K<sub>α</sub> radiation with a wavelength of λ = 1.5406 Å. Lattice parameters of leucite were refined from XRD patterns against tetragonal leucite with JCPDS card No [38-1423], space group I41/a, lattice parameters: a = b = 13.0654(7) Å and c = 13.7554(13) Å. The software for lattice parameter refinement was STOE WinXPow V2.1.

### **FT-IR Analysis**

Fourier Transform Infrared absorption spectra of the selected crystallized glass-ceramics were measured at room temperature in the wavenumber range of 4000–400 cm<sup>-1</sup> using a Fourier transform infrared spectrometer (VERTEX 7.0, Bruker). The selected crystallized glass-ceramics were ground into fine powders and then mixed with KBr powder; subsequently, the mixtures were uniaxially pressed to form clear homogeneous discs. The FT-IR measurements were carried out immediately after preparing the discs to avoid moisture absorption.

### **Microstructures**

Samples for scanning electron microscopy (SEM) analysis were ground and then polished to a mirror finish using alumina slurry (1 μm). Chemical etching was required to reveal surface microstructures where the etchant used was composed of concentrated HF (50%) 15 ml, concentrated HNO<sub>3</sub> (70%) 5 ml and deionized water 80 ml.<sup>(18)</sup> Etching was carried out at room temperature for 30 – 45 seconds. Samples were then ultrasonically cleaned and gold-

coated for conductive layer by a Cressing Sputter Coater 108 before analysis by SEM. Analysis was carried out using a Camscam SEM with EDAX link, operated at 10 – 20 kV. Backscattered electron (BE) mode was used to reveal microstructures and see qualitative changes in composition at the sample surface which had been etched.

## **Results and Discussion**

### **Thermal Analysis and Crystallization**

Quenching the glass melts in water at room temperature resulted in translucent glasses for all three compositions. The translucency might have occurred due to partial crystallization during quenching.<sup>(12, 14-15)</sup> However, fine glass powders in this study displayed the ability to crystallize and form leucite-based glass-ceramics at a later stage. Leucite had previously been crystallized in alkali aluminosilicate glasses,<sup>(10)</sup> and in this study bulk crystallization was thought to be the dominant crystallization mechanism. The addition of TiO<sub>2</sub> in the base glass compositions was intended to act as a nucleating agent given that this effect was stressed by authors in several studies.<sup>(9, 13-15)</sup>

DTA traces of as-quenched glasses A, B and C are shown in Figure 1. The thermal transitions were detected and recorded by computer software equipped with a Netzsch STA 449C DTA. The first endotherm from each glass composition (indicated by +) was detected from the slope change of derivative curve (not shown here) and corresponds to the glass transition temperature, T<sub>g</sub>. It was found that alkali silicate based glasses containing a higher amount of K<sub>2</sub>O as network modifier resulted in lower T<sub>g</sub>. The T<sub>g</sub> values were 638, 602 and 594°C for glasses A, B and C, respectively. This behavior is commonly observed in alkali silicate glasses where the glass networks are broken by non-bridging oxygen.<sup>(19- 20)</sup> Exotherms (indicated by ×) in all three glass compositions can be correlated with the crystallization of glasses to form glass-ceramics. The DTA curves in all 3 glasses showed broad humps rather than clear distinct exothermic peaks. Therefore, these curves could not easily follow crystallization from DTA curves in Figure 1. However, the derivative curves using computer software equipped with Netzsch STA 449C DTA showed changes in slope at similar positions in the temperature range 700 – 1100°C. Consequently, heat treatment was performed in this study at 850, 900, 950 and 1000°C (following DTA data) to form glass-ceramics,

assuming phase evolution was completed at each isothermal hold of 4 hours.

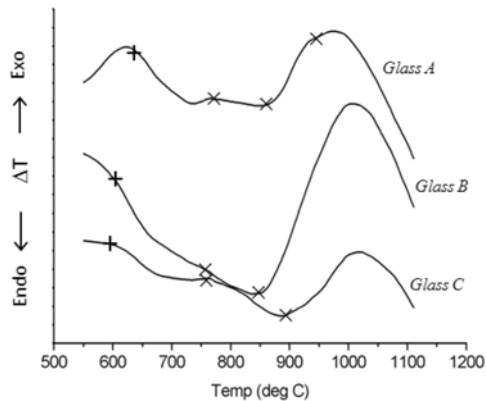


**Figure 1.** DTA traces of the as-quenched glasses A, B and C

### X-ray Diffraction

X-ray diffraction (XRD) patterns of glasses A, B and C which were heat-treated from 850 – 1000°C are shown in Figures 2, 3 and 4, respectively. In as-quenched glasses of all compositions, XRD patterns revealed some sharp peaks rather than a broad background, which gave evidence of trace amounts of crystalline phases. The XRD results confirmed the above-mentioned observation that quenching the glass melts in water at room temperature resulted in translucent glasses, and that this translucency was due to partial crystallization of glasses. Although partial crystallization occurred before the controlled crystallization process was to be carried out, the quenched glasses were mainly amorphous since the XRD patterns revealed rather broad and noisy background. Crystallization processes at 850, 900, 950 and 1000°C for glasses A (Figure 2), B (Figure 3) and C (Figure 4) all showed tetragonal leucite ( $\text{KAlSi}_2\text{O}_6$ ) as the main phase, labeled as  $\bullet$ . This phase corresponds to the JCPDS card number [38-1423]. It is evident that the amount of leucite phase in each heat-treated glass composition increased with increasing heat treatment temperatures from 850 – 950°C. This is shown by an increase in relative peak heights responsible for the leucite phase. In all heat-treated glass samples, secondary phase/s crystallized out along with the main phase. Isothermal heat treatment at 850 and 900°C for 4 hours resulted in the evolution of secondary phases which were thermodynamically metastable. These metastable phases dissolved away at higher temperatures and a more stable phase ( $\blacklozenge$ ) appeared at 950°C in all heat-treated glasses. The second phase ( $\blacklozenge$ ) was best indexed as  $\text{KAlSi}_3\text{O}_8$  (Potassium aluminum

silicate, Microcline maximum) with JCPDS card number [84-709] and has triclinic crystal structure. The crystallization of  $\text{KAlSi}_3\text{O}_8$  formed in the temperature range of 950 – 1000°C in this study was previously identified in leucite reinforced glass-ceramics in  $\text{K}_2\text{O} - \text{Al}_2\text{O}_3 - \text{SiO}_2 - \text{TiO}_2$  glass systems by Cattell, *et al.*<sup>(10, 11)</sup> They identified this minor phase as  $\text{KAlSi}_3\text{O}_8$  (sanidine) with monoclinic crystal structure. Sanidine has the same chemical formula as microcline and their crystal structures are closely related. Only glass composition C, which had higher  $\text{K}_2\text{O}/\text{SiO}_2$  ratio when heat-treated above 950°C, showed another unidentified secondary phase ( $\blacktriangle$ ). The relative peak intensities responsible for  $\blacktriangle$  and  $\blacklozenge$  became stronger for glass C heat-treated at 1000°C. This means that the relative amount of the major leucite phase decreased as the second phase/s became more important at higher heat treatment temperatures, especially in glass composition C.

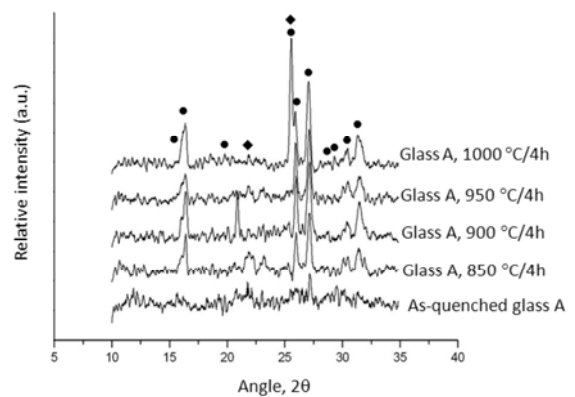


**Figure 2.** XRD patterns of as-quenched and heat-treated glass A from 850 to 1000°C.  $\bullet$  The major leucite phase ( $\text{KAlSi}_2\text{O}_6$ ) and  $\blacklozenge$  the secondary phase ( $\text{KAlSi}_3\text{O}_8$ )

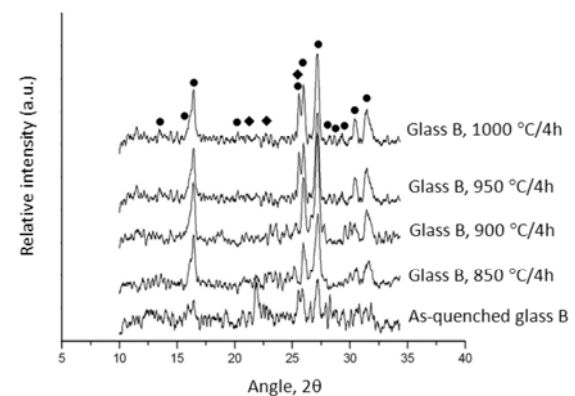


**Figure 3.** XRD patterns of as-quenched and heat-treated glass B from 850 to 1000°C  $\bullet$  The major leucite phase ( $\text{KAlSi}_2\text{O}_6$ ) and  $\blacklozenge$  the secondary phase ( $\text{KAlSi}_3\text{O}_8$ )

Effect of  $K_2O/SiO_2$  Ratio on the Crystallization of Leucite in Silicate-Based Glasses

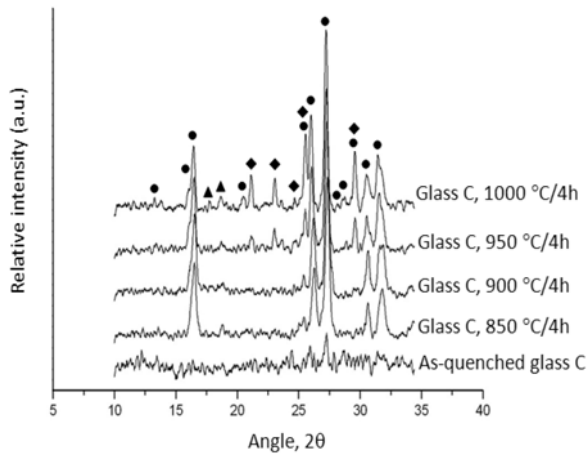


**Figure 4.** XRD patterns of as-quenched and heat-treated glass C from 850 to 1000°C. ● The major leucite phase ( $KAlSi_2O_6$ ), ◆ the secondary phase ( $KAlSi_3O_8$ ), ▲ unidentified phase

Figure 5 shows the comparison between glass A, glass B and glass C, heat-treated at 1000°C for 4 hours. As far as the peak intensities of tetragonal leucite crystals are concerned, it was found that the relative peak heights increased with increasing  $K_2O/SiO_2$  ratio and also with increasing heat treatment temperature from 850 – 900°C, thus indicating an increase in the amount of leucite phase. This finding agrees with the assumption made earlier that an increase in  $K_2O/SiO_2$  ratio would result in the crystallization of more leucite phase. Peak maxima responsible for tetragonal leucite phase were observed at a heat treatment temperature of 900°C for all base glass compositions. Above 900°C, the relative amount of leucite phase decreased. This possibly occurred due to an increase in the amount of secondary phase  $KAlSi_3O_8$ . Unit cell dimensions of the tetragonal leucite phase in the crystallized samples were refined from XRD patterns using a least-square method and are summarized in Table 2. In the crystallized samples of glass A and glass B, the  $c/a$  ratios were very similar ( $\sim 1.044$  and  $1.045$ ), but those in glass C showed a slight increase in the  $c/a$  ratio from 1.0402 to 1.0467 with increasing heat treatment temperatures from 850 – 1000°C. This means there is a slight increase in the tetragonality of the leucite phase.

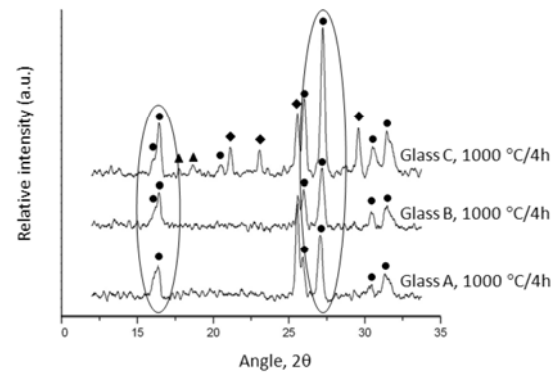


**Figure 5.** Comparison of XRD patterns for glasses A, B and C heat-treated at 1000°C/4h. ● The major leucite phase ( $KAlSi_2O_6$ ), ◆ the secondary phase ( $KAlSi_3O_8$ ), ▲ unidentified phase

**Table 2.** Refined lattice parameters and  $c/a$  ratio for the tetragonal leucite phase

Glass	Heat treatment	Unit cell dimension			Unit cell volume ( $\text{\AA}^3$ )
		a = b ( $\text{\AA}$ )	c ( $\text{\AA}$ )	c/a ( $\text{\AA}$ )	
A	850 °C	13.132(7)	13.709(8)	1.0439	2363.9(22)
	900 °C	13.133(11)	13.712(12)	1.0441	2365.0(31)
	950 °C	13.131(15)	13.709(17)	1.0440	2364.0(43)
	1000 °C	13.152(16)	13.729(18)	1.0439	2374.6(47)
B	850 °C	13.11(3)	13.70(3)	1.0450	2348.8(88)
	900 °C	13.117(8)	13.708(10)	1.0450	2358.4(25)
	950 °C	13.116(19)	13.717(22)	1.0458	2359.6(56)
	1000 °C	13.121(12)	13.711(14)	1.0450	2360.4(37)
C	850 °C	13.039(17)	13.563(20)	1.0402	2305.9(50)
	900 °C	13.043(3)	13.591(3)	1.0420	2312.3(8)
	950 °C	13.077(8)	13.675(10)	1.0456	2338.8(24)
	1000 °C	13.083(19)	13.694(22)	1.0467	2343.9(57)

Increasing the network modifying oxides, e.g.  $Na_2O$  and  $K_2O$ , can break up the silicate network, reducing the viscosity for viscous flow as discussed elsewhere.<sup>(19, 20)</sup> This would affect the nucleation and growth mechanisms in alkali aluminosilicate glasses.<sup>(9, 20)</sup> In this study, not only did glass composition with higher  $K_2O/SiO_2$  ratio lead to an increase in the amount of leucite phase crystallized out as shown earlier by XRD data, but it also led to a lower glass transition temperature,  $T_g$ , of the residual glass in the crystallized samples. This may have resulted in the easier crystallization (i.e. nucleation and crystal growth process) in glass C and a lower crystal clamping effect by the residual glass.<sup>(21, 22)</sup> It also led to an increase in the  $c/a$  ratio of the leucite phase when glass C was subjected to increasing heat treatment temperature. The previous study by Denry, *et al.*<sup>(23)</sup> suggested easier crystallization of

sanidine when glass viscosity was reduced by increased modifier content such as  $\text{Na}_2\text{O}$  and  $\text{K}_2\text{O}$  which then led to the precipitation at a temperature range of 800 – 950°C. In the current investigation, nucleation and crystallization of secondary phase in glass C may have been easier since the base glass composition contained a higher amount of  $\text{K}_2\text{O}$  as a glass network modifier and the  $T_g$  was lower. Szabo, *et al.*<sup>(24)</sup> suggested that the crystallization of sanidine phase appeared to be associated with the phase separated calcium-rich areas which may have led to a region of increased mobility. In this study, therefore, CaO may have acted as a nucleation site for  $\text{KAlSi}_3\text{O}_8$ .

### FT-IR Analysis

Glass C heat-treated at 850, 900, 950 and 1000°C/4 hours was selected for Fourier transform infrared (FT-IR) absorption analysis. The results are shown in Figure 6. Different IR absorption peaks were assigned, and correlated with the functional groups present in the samples. The results showed the effect of heat treatment temperature (at a fixed glass composition) on the numbers and positions of the absorption peaks. The results can be summarized as follows<sup>(25, 26)</sup>:

- 1) The broad absorption peaks at 3400 – 3500  $\text{cm}^{-1}$  is due to the O–H stretching of water/moisture that comes during sample preparation for FT-IR.
- 2) The small absorption peaks at about 1450 and 1600  $\text{cm}^{-1}$  are related to CO group and molecular water, respectively. The CO absorption peak might be due to chemisorption of atmospheric  $\text{CO}_2$  on the surface.
- 3) The intense broad absorption peaks at about 1000  $\text{cm}^{-1}$  and 770  $\text{cm}^{-1}$  are assigned to the asymmetric and symmetric stretching vibrations of the tetrahedral silicate network, respectively. It can hence be said that these strong absorption peaks are possibly responsible for the leucite phase.
- 4) The sharp absorption peak at about 460  $\text{cm}^{-1}$  is assigned to bending and rocking motions of the silicate network.
- 5) This investigation demonstrates plainly that the changes in the heat treatment temperature of glass C cause only small alterations in the positions or intensities of the bands. The slight shift of the wavenumbers can be correlated with the degree of polymerization of the silicate network structure.
- 6) It can be said that all heat-treated samples in the silicate network were of the same structure and could be responsible for the leucite phase.

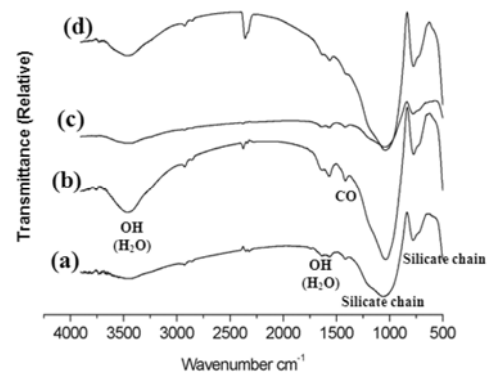


**Figure 6.** FTIR spectra of glass C heat-treated at (a) 850°C, (b) 900°C, (c) 950°C and (d) 1000°C.

### Backscattered Electron Imaging

Microstructures under backscattered electron (BE) mode of glasses A, B and C heat-treated at 1000°C/4 hours are shown in Figures 7, 8 and 9, respectively. Chemical etching on the sample surfaces was sufficient to discern microstructures, even though some residual glass within the resolution of a Camscan SEM can be observed, which resulted in unclear images. Figure 7 shows two different crystal morphologies and contrasts, rounded and rod-shaped. Qualitative elemental analysis of these two phases by Energy Dispersive X-ray Spectroscopy (EDS) showed similar traces. They comprised mainly of Al, Si and K (data not shown). It is therefore difficult to relate the EDS results to the XRD data. However, the rounded crystals may be related to the leucite phase as they possess a higher volume fraction. The rod-shaped crystals can then be related to the secondary phase ( $\text{KAlSi}_3\text{O}_8$ ). In Figure 8, crystals are of very similar morphologies to those found in Figure 7, although the rod-shaped crystals appeared larger in size. In Figure 9, the base glass composition contained higher amount of  $\text{K}_2\text{O}/\text{SiO}_2$  ratio and after crystallization at 1000°C/4 hours the etched sample revealed a rather clear microstructure. Low magnification SEM image showed plates of agglomerated crystals. An inset in Figure 9 is a higher magnification image of the zoomed area. It generally shows large volume fraction of spherical crystals with clear edges. These crystals were assumed to be tetragonal leucite since this phase appeared in large amount according to the XRD result shown in Figure 5. The rod-shaped crystals can also be observed in some areas. This phase could be associated with  $\text{KAlSi}_3\text{O}_8$ , which is the same phase found in the heat-treated glasses A and B. When comparing SEM images in Figures 7, 8 and 9, the size of rounded crystals, which was assumed to be the leucite phase, varied slightly from 2 – 5  $\mu\text{m}$  and

*Effect of  $K_2O/SiO_2$  Ratio on the Crystallization of Leucite in Silicate-Based Glasses*

became sharply edged with composition containing a higher amount of  $K_2O/SiO_2$  ratio. Heat-treated glass C also seems to give slightly larger leucite crystal size, which is presumably due to a lower crystal clamping effect.<sup>(21,22)</sup>

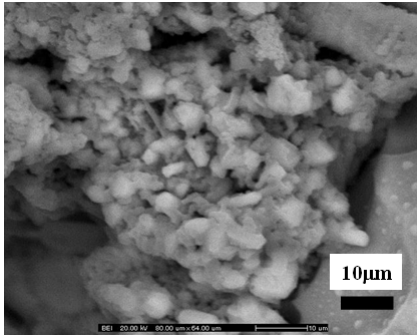


**Figure 7.** SEM image of leucite-based glass-ceramics for glass A heat-treated at 1000°C/4h.

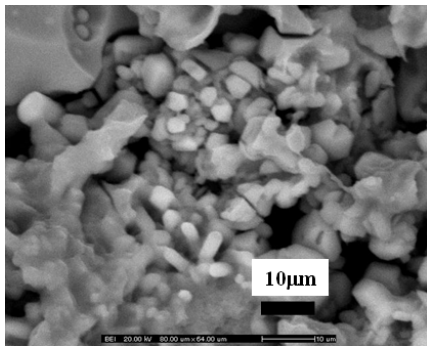


**Figure 8.** SEM image of leucite-based glass-ceramics for glass B heat-treated at 1000°C/4h.

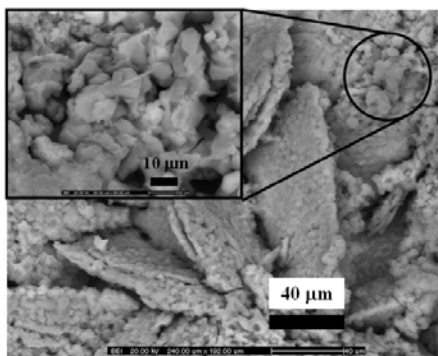


**Figure 9.** SEM image of leucite-based glass-ceramics for glass C heat-treated at 1000°C/4h.

A previous study by Holand, *et al.*<sup>(12)</sup> on the crystallization mechanisms in glass-ceramics showed that the early stages of bulk leucite growth have been due to dendrites growing in preferred crystallographic directions. A diffusion controlled

growth process at the smooth atomic-scale faceted crystal-glass interface was suggested. Later, a change in dendrite shape was owed to Ostwald ripening (coarsening) process that resulted in a highly organized coarsened leucite structure. Microstructures obtained in Holand, *et al.*<sup>(12)</sup> study consist of fine-grained crystals in micrometer regime dispersed in residual glass matrix which had been etched away. According to Mackert, *et al.*<sup>(6)</sup> fine grained glass-ceramics led to less matrix microcracking and potentially better wear resistance. They mentioned that crystallization heat treatments and powder particle sizes controlled the leucite crystal size, distribution and volume fraction for obtaining uniformly distributed fine-grained tetragonal leucite glass-ceramics for dental applications. This research paper shows that fine microstructures occurred in the proposed glass compositions after heat treatment. It could hence result in improved mechanical properties of leucite-based glass-ceramics. A further study on the mechanical properties will be carried out and assessed for potential dental applications.

## Conclusions

In this study, crystallization of glasses resulted in glass-ceramics with leucite as the major crystalline phase. As-quenched glasses showed crystallization temperatures between 700 and 1100°C. Glasses containing higher  $K_2O/SiO_2$  ratio showed lower glass transition temperatures, and after crystallization the amount of leucite phase increased more than for those with smaller  $K_2O/SiO_2$  ratios. Glass with highest  $K_2O/SiO_2$  ratio in this study showed a higher amount of secondary phase/s when heat-treated at 1000°C. Microstructures of all crystallized glass compositions at 1000°C were similar and consisted of fine crystals dispersed in glassy matrix which had been etched away. The rounded crystals, assumed to be the leucite phase, became sharply edged with composition containing a larger amount of  $K_2O/SiO_2$  ratio and were observed to be slightly larger in crystal size, probably due to lower crystal clamping effect.

## Acknowledgements

The authors would like to thank the department of Materials Science and Engineering, Silpakorn University, and the Center of Excellence for Petroleum, Petrochemicals and Advanced Materials, Chulalongkorn University, for financial support.

## References

1. Kelly, J.R. 2004. Dental ceramics: current thinking and trends. *Dent. Clin. North Am.* **48(2)** : 513–530.
2. Kelly, J.R., Nishimura, I. and Campbell, S.D. 1996. Ceramics in dentistry: historical roots and current perspectives. *J. Prosthet. Dent.* **75(1)** : 18–32.
3. Hench, L.L. 2005. Bioceramics: from concept to clinic. *J. Am. Ceram. Soc.* **74(7)** : 1487–1510.
4. Höland, W., Rheinberger, V., Apel, E. and Hoen, C. 2007. Principles and phenomena of bioengineering with glass-ceramics for dental restoration. *J. Eur. Ceram. Soc.* **27(2-3)** : 1521–1526.
5. Kelly, J. R., Campbell, S. D. and Bowen, H. K. 1989. Fracture surface analysis of dental ceramics. *J. Prosthet. Dent.* **62(5)** : 536–541.
6. Mackert, J.R., Russell, C.M. and Williams, A.L. 2001. Evidence of a critical leucite particle size for microcracking in dental porcelains. *J. Dent. Res.* **80(6)** : 1574–9.
7. Mackert, J.R., Butt, M.B. and Fairhurst, C.W. 1986. The effect of the leucite transformation on dental porcelain expansion. *Dent. Mater.* **2(1)** : 32–36.
8. Novotna, M. and Maixner, J. 2006. X-ray powder diffraction study of leucite crystallisation. *Z. Kristallogr. Suppl.* **23** : 455–459.
9. Holand, W. and Beall, G.H. 2002. *Glass-ceramic technology*. Westerville, Ohio: The American Ceramic Society : 372.
10. Cattell, M.J., Chadwick, T.C., Knowles, J.C. and Clarke, R.L. 2005. The crystallization of an aluminosilicate glass in the  $K_2O-Al_2O_3-SiO_2$  system. *Dent. Mater.* **21** : 811–822.
11. Cattell, M. J., Chadwick, T.C., Knowles, J.C., Clarke, R.L. and Samarawickrama D.Y.D. 2006. The nucleation and crystallization of fine grained leucite glass-ceramics for dental applications. *Dental. Materials.* **22(10)** : 925–933.
12. Höland, W., Frank, M. and Rheinberger, V. 1995. Surface crystallization of leucite in glass. *J. Non-Cryst. Solids.* **180(2-3)** : 292–307.
13. Höland, W. 1997. Biocompatible and bioactive glass-ceramics – state of the art and new directions. *J. Non-Cryst. Solids.* **219(1)** : 192–197.
14. McMillan, P. 1979. *Glass-ceramics*. 2<sup>nd</sup> ed. London: Academic Press Inc.
15. Beall, G. 1989. Design of glass-ceramics. *Solid State Sci.* **3** : 333–354.
16. James, P. 1982. Nucleation in glass forming systems—a review. In: *Simmons, J.H., Uhlmann, D.R., Beall, G. (eds) Advances in ceramics, nucleation and crystallisation in glasses*. Columbus, Ohio: The American Ceramic Society.
17. Grossman, D.G. 1985. Cast glass-ceramics. *Dent. Clin. North Am.* **29** : 719–723.
18. Sooksaen, P. and Reaney, I.M. 2008. Thermal analysis and phase evolution of ferroelectric  $PbTiO_3$  obtained from silicate and borate based glasses. *J. Mater. Sci.* **43(4)** : 1265–1269.
19. Doremus, R.H. 1994. *Glass science*. 2<sup>nd</sup> ed. New York: Wiley.
20. Shelby, J.E. 2005. *Introduction to glass science and technology*. 2<sup>nd</sup> ed. Cornwall: TJ International.
21. Grossman, D.G., and Isard, J.O. 1969. Crystal clamping in  $PbTiO_3$  glass-ceramics. *J. Mater. Sci.* **4** : 1059.
22. Sooksaen, P., Reaney, I.M. and Sinclair, D.C. 2005. Lead titanate glass-ceramics derived from a silicate-based melt. *J. Mater. Res.* **20(5)** : 1316–1323.
23. Denry, I.L., Holloway, J.A. and Colijn, H.O. 2001. Phase transformations in a leucite-reinforced pressable dental ceramic. *J. Biomed. Mater. Res.* **54(3)** : 351–359.



*Effect of K<sub>2</sub>O/SiO<sub>2</sub> Ratio on the Crystallization of Leucite in Silicate-Based Glasses*

24. Szabo, I., Nagy, B., Völksch, G. and Höland, W. 2000. Structure, chemical durability and microhardness of glass-ceramics containing apatite and leucite crystals. *J. Non-Cryst. Solids*. **272(2-3)** : 191–199.
25. Elliott, J.C. 1994. *Structure and chemistry of the apatites and other calcium orthophosphates*. Amsterdam :Elsevier Science.
26. Kuriakose, T.A. and Kalkura, S.N. 2004. Synthesis of stoichiometric nano crystalline hydroxyapatite by ethanol-based sol–gel technique at low temperature. *J. Cryst. Growth*. **263(1-4)** : 517–523.